Supporting Information

Wälchli et al. 10.1073/pnas.1216203110

SI Materials and Methods

Mice. We used WT and Nogo-A$^{-/-}$ C57BL/6 mice (1). All animal experiments were approved by the Cantonal Veterinary Department of Zurich (license no. 1732010).

Antibodies. Neutralizing anti–Nogo-A antibody 11C7 was raised against an 18-amino acid Nogo-A peptide corresponding to the rat sequence amino acids 623–640 (within the Nogo-A Delta 20 fragment) (2) (a gift from Novartis Pharma, Basel) and produced in large quantity. As a control antibody, an IgG1 directed against BrdU (AbD Serotec) was used.

Intraperitoneal Antibody Injections. Postnatal day 0 (P0) WT mice were daily injected i.p. with 11C7 (2, 3) or the control IgG at a final dose of 20 $\mu g \cdot g^{-1}$ body weight. At day P8, animals were transcardially perfused with 0.1 M PBS (pH 7.4) followed by 4% (wt/vol) paraformaldehyde (PFA) in 0.1 M PBS. Mouse antibody penetration into the CNS tissue was confirmed using an anti-mouse IgG and the ABC peroxidase complex (Elite; Vector) on 40-μm free-floating sections.

Intracerebroventricular Injections of Adeno-Associated Virus Serotype 8. Adeno-associated virus serotype 8 (AAV8) containing the shRNA sequence to *Nogo-A*/*Rtn4a* or that of *gfp* was produced as previously described (4, 5). One microliter of AAV8 (10^{13} vg/mL) was injected in each cerebral ventricle of three P0 mice. Mice were perfused with 4% (wt/vol) PFA in 0.1 M PBS at P8, and 20-μm-thick cortical brain sections were cut for blood vessel analysis.

Immunofluorescence Staining and Analysis of Postnatal Brain Angiogenesis. After perfusion with 0.1 M PBS followed by 4% (wt/vol) PFA in 0.1 M PBS, P8 brains were removed, postfixed, and frozen in Tissue-Tek (Sakura), and 20-μm coronal cryostat sections were stained for isolectin B4 (IB4) from *Griffonia simplicifolia* conjugated to Alexa Fluor 594 (Invitrogen/Molecular Probes) in a 1:100 dilution in 0.1 M PBS containing 0.03% Triton X-100 at 4 °C overnight. The sections were washed with 0.1 M PBS, stained with DAPI and were mounted using Mowiol (Mowiol 4-88, Sigma-Aldrich). Inverted microscope images of brain sections were used to analyze vessel density based on a stereological grid method described below. Four mice of each genotype or treatment group were used for quantifications.

Immunofluorescence Staining and Analysis of Postnatal Retinal Angiogenesis. Visualization of retinal vessels was performed as described (6) with minor modifications. Briefly, after perfusion (see above) P4/P8 retinas were dissected carefully, cut, stained with IB4 and the following primary antibodies, respectively: rabbit anti-Nogo-A [Laura (2); 1:250], mouse anti-βIII tubulin (1:500; Promega), rat anti-PDGF receptor β (PDGFRβ) (1:100; eBioscience), and rabbit anti-GFAP (1:1,000; DAKO) as described above and were flat-mounted with Mowiol. Confocal microscope images of retinal flat mounts were used to analyze the vessel density (based on a stereological grid method described below) or to analyze the length of radial migration and the vessel coverage. Four to seven mice of each genotype or treatment group were used for quantifications.

Analysis of Postnatal Brain and Retinal Vessel Density. A stereological grid (7) consisting of squares with side lengths of 50 μm was superimposed on digital images of brain sections and retina flat mounts (deeper layer) stained for IB4. The relative density of blood vessels in the tissue (= tissue vessel density) was calculated on each section by dividing the number of points falling on blood vessel structures by the total number of points falling on the sampling area using ImageJ.

For a given brain region (cortex, hippocampus, corpus callosum, and superior colliculus), six to eight sections per animal were analyzed. For retinal flat mounts (deeper layer), four retinal quadrants per animal were analyzed.

For the superficial retinal layer, vascular density was measured by calculating the areas covered by vessels in all four quadrants in each retina using ImageJ. The radial length of the vascular network was measured based on the average length of at least 10 lines drawn from the center of the retina in the optic disk to the edge of the vascular plexus. For every brain region, four brains from each genotype were analyzed. Four to seven retinas from each genotype were used for all quantifications (superficial and deeper retinal layer).

Analysis of Evans Blue-Perfused Vessels. The number of perfused blood vessels was assessed according to a previously described method (8, 9) by intracardial injection of 2% (wt/vol) Evans blue (Sigma) (6 uL/g) dissolved in 0.9% NaCl during isoflurane anesthesia of P8 and adult WT and Nogo-A$^{-/-}$ mice. For antibody-treated animals, Evans blue was injected intracardially at the day of the last i.p. antibody injection (P8). Heads were cut and frozen, and 10-μm coronal cryosections were fixed, dehydrated in acetone at −25 °C for 1 min, and transferred to room-temperature acetone. After coverslipping, sections were photographed using a fluorescence microscope (AxioImager2; Zeiss), and the position of each photograph was stored by a computer-controlled microscope stage. Then the coverslips were removed and sections were rehydrated in a humid chamber at 4 °C overnight and stained with Alexa 594-labeled IB4 [1:100 in 0.1 M PBS (pH7.4) containing 0.3% Triton X-100 for 1 h]. Next, the areas already photographed with the Evans blue fluorescence were relocalized using the computer-controlled microscope stage and were photographed for the IB4 signal. The number of Evans blue-perfused and of IB4-labeled blood vessels was determined using an image-analyzing system MCID (Ontario Research).

Immunofluorescence Microscopy of Brain Sections and of Cortical Endothelial Tip Cells. P4/P8 40-μm coronal free-floating sections were postfixed for 10 min in either 4% (wt/vol) PFA in 0.1 M PBS (P8 animals) or in 4% (wt/vol) PFA, 0.05% glutaraldehyde in 0.1 M PBS (P4 animals). Antigen retrieval was performed by incubating the sections in 50 mM NH_4Cl in 0.1 M phosphate buffer for 30 min, 50 mM glycine in 0.1 M Tris (pH 8.0) for 5 min at 80 °C, and subsequent microwave heating in $CaCl_2$-containing buffer [0.1 mM $CaCl_2$ 0.1 mM $MgCl_2$ 0.1 mM MnCl diluted in 0.1 M PBS (pH 6.8), slightly modified according to ref. 3]. After permeabilization in 0.1 M Tris-buffered saline and 0.3% Triton X-100 for 10 min at room temperature, the sections were incubated for 72 h at 4 °C in primary antibodies diluted in $CaCl_2$-containing buffer, 0.05% Triton X-100, and 2% (vol/vol) normal goat serum (NGS) in 0.1 M PBS using the following primary antibodies or biotinylated IB4, respectively: rabbit anti–Nogo-A (Laura (6), 1:250), mouse anti-βIII tubulin (1:500; Promega), rabbit anti-glucose transporter 1 (anti–GLUT-1) (1:250; Millipore), rat anti-PDGFRβ (1:200; eBioscience), rabbit anti-GFAP (1:1,000; DAKO Cytomation), mouse anti-NeuN (1:500; Millipore), DAPI (1:40,000), and biotinylated IB4 (20 $\mu g \cdot mL^{-1}$; Sigma).

After incubation with primary antibodies, the sections were washed and incubated with secondary antibodies (goat anti-rabbit, goat anti-mouse, 1–2 $\mu g \cdot mL^{-1}$) or streptavidin-Alexa Fluor 594 conjugate (1:200; Jackson Laboratories) diluted in $CaCl_2$-containing buffer as described above before mounting with Mowiol. Images were acquired using a Leica SP2 or an OLYMPUS confocal microscope, and IMARIS software was used for 3D reconstruction of confocal *z*-stacks.

Endothelial tip cell quantification was performed on 40-μm free-floating sections in bregma-matched, defined cortical areas including cingulate and motor cortex using a Leica SP2 confocal microscope (40× oil objective, NA1.25). The areas of the analyzed cortical regions were measured using ImageJ software, and the number of tip cells was normalized to the corresponding cortical area. Tip cells were defined as $IB4^+$ structures with a typical, tip cell-like shape and five or more filopodia, according to previous reports (6, 10). For each genotype, at least two sections from at least three animals were analyzed.

Isolation and Culture of Brain-Derived Microvascular Endothelial Cells. Microvascular endothelial cells (MVECs) were prepared and cultured according to ref. 11. Briefly, the P8 WT mice brains were dissected, meninges, large vessels, and choroid plexus were removed, and MVECs were isolated as described. Every 2–3 d, the MVEC medium [DMEM + 4.5 $mg \cdot mL^{-1}$ D-glucose, 2 mM *N*-acetyl-L-alanyl-L-glutamine, 50 $\mu g \cdot mL^{-1}$ gentamycin, 20% (vol/vol) FCS, 100 $\mu g \cdot mL^{-1}$ endothelial cell growth supplement (SERVA), and 16 units/mL heparin (Sigma)] was replaced, and cells were used at passage 1–3.

The purity of endothelial cell cultures was assessed by immunofluorescence using an anti-von Willebrand factor antibody (1:500; DAKO) and was found to be ≥90%.

PC12 Culture. PC12 cells were cultured in PC12 medium [DMEM plus 4.5 $mg \cdot l^{-1}$ D-glucose, 2 mM *N*-acetyl-L-alanyl-L-glutamine, 50 $\mu g \cdot mL^{-1}$ gentamycin, 6% (vol/vol) newborn calf serum, and 6% (vol/vol) horse serum].

Preparation of P10 Mouse Brain Extracts. Brain membrane protein extracts were obtained from WT and Nogo-$A^{-/-}$ P10 mice according to refs. 2 and 12.

Briefly, the brain extracts were homogenized directly in 3-[(3-cholamidopropyl)dimethylammonio]-1-propanesulfonate (CHAPS) extraction buffer (50% or 100% wt/vol) and were centrifuged twice at 100,000 × *g* (using a Beckman TL-100 Ultracentrifuge, fixed angle) for 1 h at 4 °C. Finally, clear supernatant was aliquoted, frozen in liquid nitrogen, and stored at −80 °C until protein determination (BioRad DC, Protein Assay) and use.

Spreading Assay. Spreading of MVEC cells was determined as described previously for 3T3 fibroblasts (2). The role of the Ras homolog gene family, member A (Rho-A)-Rho-associated, coiled-coil containing protein kinase (ROCK) pathway was addressed by the treatment of MVECs with the specific ROCK inhibitor Y27632 (20 μM) (Sigma-Aldrich). Spreading experiments on mouse brain extracts of P10 WT or Nogo-$A^{-/-}$ mice were performed by coating four-well Petri dishes (Greiner BioOne; well area: 1 cm^2) with brain extracts at various concentrations. Plates were washed, and the MVEC spreading experiment was performed as described above. For neutralization experiments, 11C7 or control IgG was added at 20 $\mu g \cdot mL^{-1}$ 1 h before MVEC addition and during the experiment. Analysis of the percentage of cell spreading was performed using an inverted microscope (Olympus Camedia C-7070) by determining the ratio between spread MVECs and the total number of adhered MVECs in three randomly chosen high-power fields in each well. The percentage of cell adhesion was determined by analyzing the ratio between the number of adhered MVECs on a given concentration of Nogo-A Delta 20 in a coated dish and the number of adhered MVECs in the PBS control dish.

Each experiment was performed at least three times in three replicate wells, and cell spreading and adhesion were quantified manually. F-actin was visualized with FITC-conjugated phalloidin (1:100; Invitrogen).

Transmigration Assay. The undersides of the 24-well plate inserts (FluoroBlock; BD Falcon) were coated for 1 h at 37 °C with 0.5 mL PBS containing 10 $\mu g \cdot mL^{-1}$ fibronectin (recombinant mouse fibronectin; Biopur AG) and different concentrations of Nogo-A Delta 20, Nogo-A Delta 21, and Nogo-66, respectively. MVECs were starved in migration medium (DMEM + 0.25% BSA) for 4 h before detachment with Accutase (PAA Laboratories). Cells were resuspended in migration medium (1 $Mio \cdot mL^{-1}$) and were labeled with calcein AM (4 $\mu g \cdot mL^{-1}$) (Molecular Probes), followed by washing with HBSS and resuspension in migration medium (125,000 $cells \cdot mL^{-1}$). The coated inserts were washed, and the bottom chamber was prepared by adding migration medium with or without mouse VEGF-A (10 $ng \cdot mL^{-1}$) (PeproTech Inc.). The inserts then were put in an empty 24-well plate (BD Falcon), and labeled MVECs (50,000 per insert) were added.

The loaded inserts were transferred to the prepared cluster plate and incubated at 37 °C, 5% CO_2 for 4 h. A cell-titration plate was prepared by adding different numbers of cells (25,000/12,500/6,250/3,125/1,563/782 cells per well) in 1.2-mL migration medium followed by incubation. The fluorescence was measured after 4 h by cytofluorimetry (Cytofluor 2350; Millipore), and the number of migrated cells was calculated based on the titration curve.

Sprouting Angiogenesis Assay. A 3D in vitro sprouting angiogenesis assay was performed as described previously (13, 14). Briefly, MVECs were mixed with 175-μm Cytodex-3 microcarrier beads (Amersham Biosciences) in MVEC medium at a ratio of 1.2×10^6 cells per 6,000 beads and were incubated for 3 h (37 °C, 5% CO_2 with shaking at regular time intervals). To ensure complete coverage of the beads with MVECs, the MVEC-bead mixture then was incubated on a tilt shaker overnight (37 °C, 5% CO_2). The next day, these cell-laden beads were washed twice in DMEM and were resuspended in DMEM + fibrinogen (1 $mg \cdot mL^{-1}$) (Sigma) + fibronectin (0.1 $mg \cdot mL^{-1}$) (BD Biosciences) containing no additive, a combination of the human angiogenic factors FGF-2 (50 $ng \cdot mL^{-1}$) (R&D Systems) and VEGF-A (60 $ng \cdot mL^{-1}$) (R&D Systems), or a combination of FGF-2/VEGF-A with Nogo-A Delta 20 or Nogo-A Delta 21 at 1 μM, respectively. This medium was cross-linked by the addition of thrombin (1 $U \cdot mL^{-1}$) (Sigma) in 48-well plates and was allowed to gel for 30 min before the addition of DMEM + 15% (vol/vol) FBS + antibiotics–antimycotics (A-A) (Gibco). After 2 d, the samples were fixed with 4% (wt/vol) PFA and imaged using a Nikon Diaphot 300 phase-contrast microscope (Nikon) fitted with a Hamamatsu digital camera (Hamamatsu Photonics). Images were analyzed for three components of sprout growth. The mean number of sprouts per bead was determined by counting the number of sprouts originating directly from the cell lining of the beads. The mean number of branch points per bead represents the number of bifurcations in the sprouts per bead. The mean total length of sprouts per bead is the total sprout length measured for each bead.

Encounter Assay. PC12 cells labeled with PKH67 (4 μM) (Sigma-Aldrich) were added in 0.5 mL PC12 medium (25,000 $cells/cm^2$), to poly-D-lysine–coated 24-well plates (BD BioCoat) or collagen I-coated ibidi eight-well plates (ibiTreat; Ibidi) and were cultured overnight. For neutralization experiments, 11C7 or control IgG (both at 20 $\mu g \cdot mL^{-1}$) was added in 50 μL MVEC medium 1 h before and simultaneously with the addition of MVEC cells labeled with PKH26 (4 μM) (Sigma-Aldrich) (25,000 $cells/cm^2$) in 0.1 mL MVEC medium. For knockdown experiments, PC12 cells were cultured on collagen I-coated ibidi eight-well plates

and were infected with 25 multiplicity of infection of Ad.shRNA Nogo-A or Ad.scrambled for 3 d before the addition of PKH26-stained MVECs. PKH67-labeled PC12 cells were cultured overnight, and PKH26-labeled cells were added the next day as described above. The cocultures were incubated, and time-lapse imaging series were acquired over 4–28 h using an inverted microscope (Leica LX; Leica) with a motorized stage. Subsequently, the time-lapse imaging series were processed and analyzed using IMARIS software (version 7.6.1). Zones of inhibition formed by MVEC cells around PC12 cells were defined as MVECs forming a circular shape around at least one PC12 cell. Zones of inhibition were addressed using inverted microscopes (AxioCam MRc; Carl Zeiss and Leica LX; Leica), and the resulting images analyzed using an AxioVision program or IMARIS software (version 7.6.1). For each condition, 42–60 positions were imaged and analyzed for zones of inhibition using a 10× objective, NA= 0.3.

Droplets Encounter Assay. Twenty thousand MVECs labeled with PKH26 (4 μM) (Sigma-Aldrich) were seeded in a 10-μL droplet on 60-mm collagen I-coated petri dishes (BD Biocoat), and 20,000 PC12 cells labeled with PKH67 (4 μM) (Sigma-Aldrich) were seeded in another 10-μL droplet at a distance of 1–2 mm. After adherence (3–4 h), cells were washed, and 3 mL of MVEC medium containing either 10 $\mu g \cdot mL^{-1}$ 11C7 or control IgG was added.

The cocultures were incubated and analyzed after 24–66 h. The migration front, where MVEC encountered PC12 cells, was addressed using an inverted microscope (Zeiss Axiovert 100). To quantify the mixture between MVEC and PC12 cells, grids were centered at the encounter of the migration fronts, and the MVECs that migrated into the PC12 droplet were counted using ImageJ.

Nanopillar Arrays. Nanopillars were fabricated from the polymeric photoresistant SU8 (MicroChem) (15, 16). Briefly, the silicon nanopillar arrays were fabricated by nanosphere lithography followed by plasma etching. Polydimethylsiloxane (PDMS) was used to replicate the inverse structure, and SU8 polymeric nanopillars were obtained by filling SU8 liquid into PDMS molds, followed by hardening through UV exposure. The spring constant k of a nanopillar as calibrated by atomic force microscopy was 79 $nN \cdot mm^{-1}$. To enable MVEC culture on nanopillars, arrays were placed on petri dishes. MVECs on nanopillars deflected the nanopillar tips (displacement x). The resulting forces exerted by MVECs was deduced using Hooke's law: $F = k^*x$.

MVEC Generation of Traction Force and Time-Lapse Video Microscopy on Nanopillar Substrates. For time-lapse experiments, MVECs (10^4 $cells \cdot mL^{-1}$) labeled with Vybrant Dil (1:200) (Invitrogen) were seeded on the nanopillar arrays and the imaging began 1 h after seeding. During image processing, MVECs were kept at constant conditions (37 °C and 10% CO_2). The fluorescent images were acquired using the lasers wavelength of 488 nm to image the nanopillars and 546 nm to image the labeled MVECs.

To measure quantitatively the effects of Nogo-A on adhesion between MVECs and nanopillars, the nanopillars were coated with different concentrations of Nogo-A Delta 20, Nogo-A Delta 21, and Nogo-66 (R&D Systems). To calculate the traction force exerted by MVECs on the nanopillar substrate, a Leica confocal microscope SP5 (63×, oil immersion, NA1.43) was used to measure the deflection of the nanopillar tips. To calculate the total mean force applied by MVECs on the substrates, the average of the displacements of 800–5,000 nanopillars per MVEC was used. Single MVECs were imaged for a total time of 20 min, with a scanning ratio of 30 s per frame. For each condition, at least three individual MVECs were analyzed. To probe how the molecular signaling as induced by Nogo-A Delta 20 is altered by inhibitors, MVECs were incubated with blockers of Rho (C3 transferase 2 μM) (Cytoskeleton Inc.), ROCK (20 μM) (Y27632; Sigma-Aldrich), Myosin II ATPase (Blebbistatin; 30 μM) (Sigma-Aldrich), and MLCK (ML-7; 20 μM) (Sigma-Aldrich) for 30 min before culture on the nanopillar substrate coated with Nogo-A Delta 20.

To study acute effects of Nogo-A on MVEC retraction, the nanopillar surface was coated with 25 $\mu g \cdot mL^{-1}$ human fibronectin for 30 min and then was washed with PBS. Subsequently, 1,1′-dioctadecyl-3,3,3′3‴-tetramethylindocarbocyanine perchlorate (DiI)-labeled MVECs were cultured for 30 min on the nanopillars and then were treated with 1 μM soluble Nogo-A Delta 20, Nogo-A Delta 21, or Nogo-66 (R&D Systems) respectively. Single MVECs then were imaged for a total time of 1.5 h, with a scanning ratio of 30 s per frame. The nanopillar displacements were recorded as sequence images when the MVECs applied forces on the nanopillar surface. For each condition, at least three individual MVECs were analyzed. To ask how co-signaling of soluble Nogo-A Delta 20 and of inhibitors affect cell functions, DiI labeled MVECs were cultured for 30 min on the nanopillar substrate before incubating the cells for another 30 min with blockers of Rho (C3 transferase; 2 μM) (Cytoskeleton Inc.), ROCK, (Y27632; 20 μM) (Sigma-Aldrich) and Myosin II ATPase (Blebbistatin; 30 μM) (Sigma-Aldrich), or MLCK (ML-7; 20 μM) (Sigma-Aldrich). Subsequently, soluble Nogo-A Delta 20 was added.

The displacements (x) of the nanopillar tips induced by whole MVECs or by single MVEC filopodia were measured later using the program Diatrack 3.03 (Powerful Particle Tracking; Semasopht). Finally, corresponding traction forces (F) were calculated using the formula $F = k^*x$, where k represents the spring constant of the nanopillars, 79 nN/μm.

Immunoblotting. Western blot analysis was performed as previously described (17). Briefly, 50-μg cell and brain tissue lysates in SDS buffer were separated on a 4–12% Bis-Tris gel (NuPage; Invitrogen) and were transferred to 0.2-μm-pore nitrocellulose membrane (NuPage, Invitrogen). After blocking with Tris buffered saline Tween (TBST) 5% (wt/vol) skim milk, the primary antibodies anti-Nogo-A Ab [Bianca (6)]; 1:10,000), anti-glycosylphosphatidylinositol (GPI)-linked leucine rich repeat (LRR) protein Nogo receptor 1 (NgR1) (R&D systems, 1:200), anti-Leucine rich repeat and Ig domain containing 1 (Lingo1) (abcam, 1:200) and anti-GAPDH (1:20,000) were incubated at 4 °C overnight, followed by the secondary antibodies (HRP conjugated anti-rabbit IgG, Jackson Immunoresearch, 1:10,000) for 1 h at room temperature. Visualization was performed using ECL solution and a chemiluminescence film (both from Amersham Bioscience).

To detect phospho-VEGFR2 and total VEGF receptor 2 (VEGFR2) proteins, 20 μg of whole-brain homogenate or MVEC lysate proteins were resolved by electrophoresis. The antibodies used were rabbit anti-VEGFR2 (1:1,000; Cell Signaling) and rabbit anti–phospho-VEGFR2 (1:1,000; Cell Signaling). To generate MVEC lysates, MVECs were starved overnight in serum-free medium. The next day, MVECs were stimulated with soluble Nogo-A Delta 20 at a final concentration of 1 μM for 5, 10, 30, or 60 min before the generation of MVEC lysates.

Quantitative Real-Time PCR. P8 brains of WT and Nogo-$A^{-/-}$ mice were dissected rapidly in RNA Later solution (Ambion), placed in Eppendorf tubes, flash frozen in liquid nitrogen, and stored at −80 °C until RNA extraction. Total RNA was prepared using the RNeasy RNA isolation kit (Qiagen) including a DNase treatment to digest residual genomic DNA. For reverse transcription, equal amounts of total RNA were transformed by oligo(dT) and M-MLV reverse transcriptase (Promega). Ten nanograms of cDNA were amplified in the Light Cycler 480 thermocycler (Roche Diagnostics AG) with the polymerase ready mix (SYBR Green I Master; Roche Diagnostics AG). The following primer pairs were designed to span intronic sequences or to cover exon-intron boundaries: *Vegfa* forward, 5′-TACTGCTGTACCTCC-ACCAT; reverse, 3′-TAGCTTCGCTGGTAGACATC; *Vegfr2*

forward, 5′-AAGCAAATGCGCAGCAGGATG; reverse, 3′-TCCTCTTCCATGCTCAGTGTCTC; *Notch4*, forward, 5′-CGTCCTGGTTTCACAGGTCAAC; reverse, 3′-TGTCCAGGTTGGCACATGTTGG; Delta-like ligand 4 (*Dll4*) forward, 5′-AGGTGCCACTTCGGTTACACAG; reverse, 3′-AGGCTCCTGCCTTATACCTCTG; *Gapdh*, forward, 5′- CAGCAATGCATCCTGCACC; reverse, 3′-TGGACTGTGGTCATGAGCCC.

The analysis of the melting curve for each amplified PCR product and the visualization of the PCR amplicons on 2% (wt/vol) agarose gels allowed the specificity of the amplification to be controlled. Relative quantification was calculated using the comparative threshold cycle ($\Delta\Delta^{CT}$) method. cDNA levels were normalized to *Gapdh* (reference gene), and a control sample (calibrator set to 1) was used to calculate the relative values.

1. Simonen M, et al. (2003) Systemic deletion of the myelin-associated outgrowth inhibitor Nogo-A improves regenerative and plastic responses after spinal cord injury. *Neuron* 38(2):201–211.
2. Oertle T, et al. (2003) Nogo-A inhibits neurite outgrowth and cell spreading with three discrete regions. *J Neurosci* 23(13):5393–5406.
3. Liebscher T, et al. (2005) Nogo-A antibody improves regeneration and locomotion of spinal cord-injured rats. *Ann Neurol* 58(5):706–719.
4. Pradhan AD, et al. (2010) Dendritic spine alterations in neocortical pyramidal neurons following postnatal neuronal Nogo-A knockdown. *Dev Neurosci* 32(4):313–320.
5. Pernet V, Schwab ME (2012) The role of Nogo-A in axonal plasticity, regrowth and repair. *Cell Tissue Res* 349(1):97–104.
6. Gerhardt H, et al. (2003) VEGF guides angiogenic sprouting utilizing endothelial tip cell filopodia. *J Cell Biol* 161(6):1163–1177.
7. Vasudevan A, Long JE, Crandall JE, Rubenstein JL, Bhide PG (2008) Compartment-specific transcription factors orchestrate angiogenesis gradients in the embryonic brain. *Nat Neurosci* 11(4):429–439.
8. Göbel U, Theilen H, Kuschinsky W (1990) Congruence of total and perfused capillary network in rat brains. *Circ Res* 66(2):271–281.
9. Theilen H, Schröck H, Kuschinsky W (1993) Capillary perfusion during incomplete forebrain ischemia and reperfusion in rat brain. *Am J Physiol* 265(2 Pt 2):H642–H648.
10. Gerhardt H, et al. (2004) Neuropilin-1 is required for endothelial tip cell guidance in the developing central nervous system. *Dev Dyn* 231(3):503–509.
11. Wachtel M, et al. (2001) Down-regulation of occludin expression in astrocytes by tumour necrosis factor (TNF) is mediated via TNF type-1 receptor and nuclear factor-kappaB activation. *J Neurochem* 78(1):155–162.
12. Spillmann AA, Amberger VR, Schwab ME (1997) High molecular weight protein of human central nervous system myelin inhibits neurite outgrowth: An effect which can be neutralized by the monoclonal antibody IN-1. *Eur J Neurosci* 9(3):549–555.
13. Nakatsu MN, Hughes CC (2008) An optimized three-dimensional in vitro model for the analysis of angiogenesis. *Methods Enzymol* 443:65–82.
14. Nakatsu MN, Davis J, Hughes CC (2008) Optimized fibrin gel bead assay for the study of angiogenesis. *J Vis Exp* 443:65–82.
15. Shiu JY, Kuo CW, Chen P (2004) Actively controlled self-assembly of colloidal crystals in microfluidic networks by electrocapillary forces. *J Am Chem Soc* 126(26):8096–8097.
16. Kuo CW, et al. (2010) Polymeric nanopillar arrays for cell traction force measurements. *Electrophoresis* 31(18):3152–3158.
17. Joset A, Dodd DA, Halegoua S, Schwab ME (2010) Pincher-generated Nogo-A endosomes mediate growth cone collapse and retrograde signaling. *J Cell Biol* 188(2):271–285.

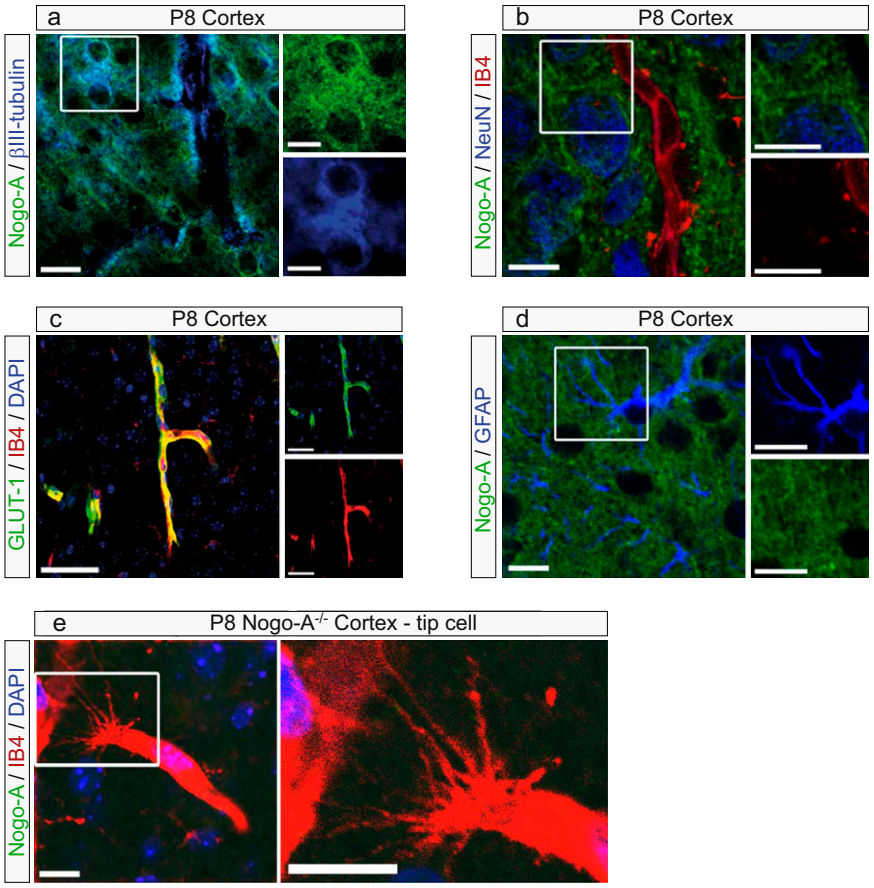

Fig. S1. Neurons expressing Nogo-A are in close proximity to blood vessels in the postnatal brain. Coronal sections (40 μm) of P8 mouse brains were stained for Nogo-A (green), the vascular endothelial cell markers IB4 (red), and GLUT-1 (green), the neuronal markers βIII-tubulin (blue) and NeuN (green), and the general nuclear marker DAPI (blue). (*A*) βIII-tubulin$^+$ neurons (blue) express Nogo-A (green) in the P8 mouse cortex. The boxed area is enlarged at right. (*B*) In the P8 mouse cortex, Nogo-A (green) is expressed in the cytoplasm of NeuN$^+$ neurons (blue) in vicinity of IB4$^+$ blood vessel endothelial cells (red). The boxed area is enlarged at right. (*C*) IB4$^+$ (red) blood vessels in the cortex at P8 express the cerebral vessel-specific endothelial marker GLUT-1 (green); DAPI staining is blue. (*D*) GFAP$^+$ astrocytes (blue) do not express Nogo-A (green) in the cortex at P8. The boxed area is enlarged at right. (*E*) Nogo-A staining (green) is not detected in the cortex of a P8 Nogo-A$^{-/-}$ mouse. The IB4-labeled endothelial tip cell and its filopodia are shown as red and DAPI$^+$ cell nuclei as blue. The boxed area is enlarged at right. (Scale bars: 20 μm in *A* and *C*–*E*; 50 μm in *C*; 10 μm in the enlarged views in *A*–*E*.)

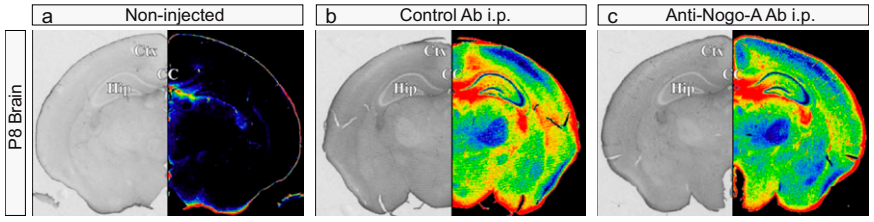

Fig. S2. The presence of control and anti–Nogo-A antibody in the P8 mouse brain after i.p. injection. Control or anti–Nogo-A purified IgG antibodies (20 μg/g body weight) were injected i.p. daily into WT mice from P0–P8. (*A*) Noninjected brain. (*B* and *C*) Control (*B*) and anti–Nogo-A antibodies (*C*) penetrated well and to a similar extent into the P8 brain parenchyma as shown by the bright-field anti-mouse immunoperoxidase staining (left side of every image) and the quantitative false color-coded densitometry (right side of every image). Dark blue represents background, and red represents maximal staining intensity. CC, corpus callosum; Ctx, cortex; Hip, hippocampus.

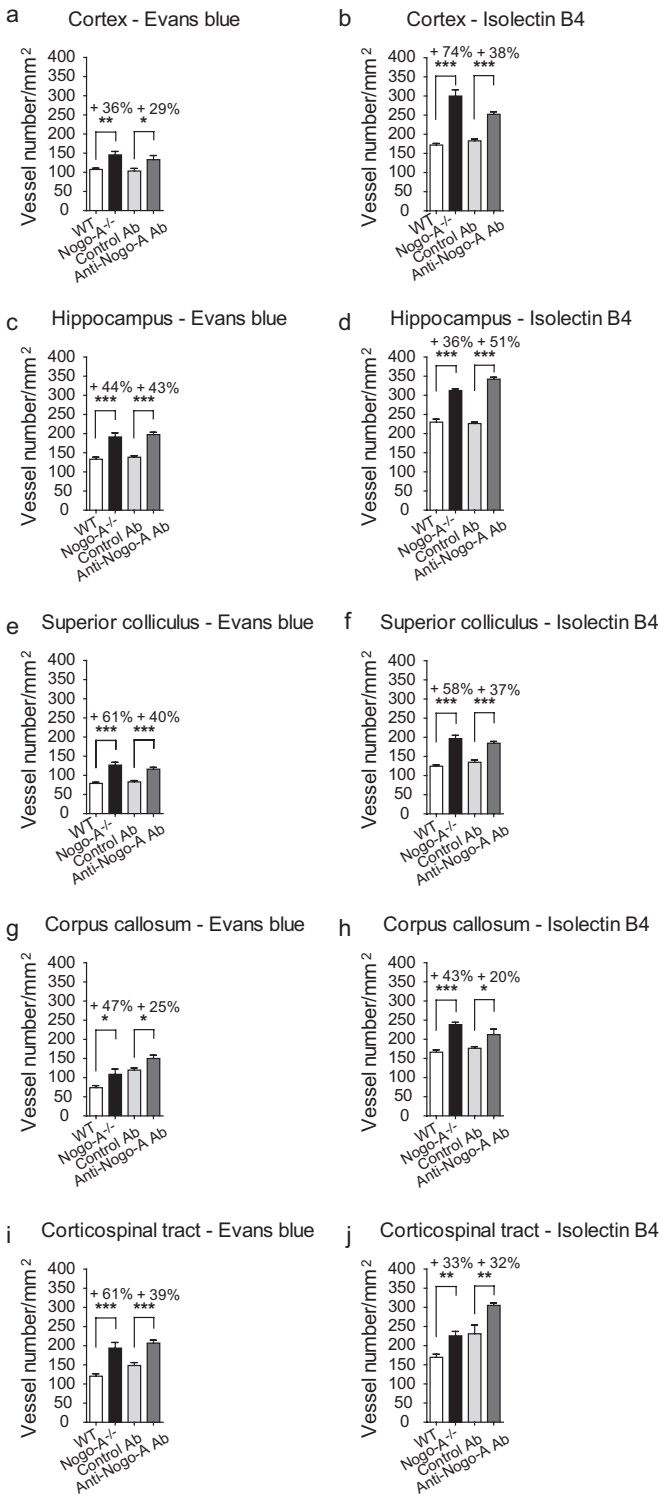

Fig. S3. Nogo-A ablation or neutralization leads to increased numbers of perfused blood vessels in the postnatal brain. Evans blue [2% (wt/vol)] in 0.9% NaCl (6 μL/g body weight) was injected into the animal's heart and perfused for 5 min before the animal's head was removed and frozen and 10-μm cryosections were prepared. (*A*, *C*, *E*, *G*, and *I*) Shown are the number of perfused (Evans blue$^+$) vessels per area in P8 cortex (*A*), hippocampus (*C*), superior colliculus (*E*), corpus callosum (*G*), and corticospinal tract (*I*) of WT mice, Nogo-A$^{-/-}$ mice, WT mice treated with the control antibody, and WT mice treated with the anti–Nogo-A antibody. Data are shown as mean ± SEM (n = 4–7). Absence of functional Nogo-A led to significantly higher numbers of blood vessels, showing that the additionally formed vessels are functional, perfused vessels. (*B*, *D*, *F*, *H*, and *J*) Shown are the number of IB4$^+$ vessel structures in P8 cortex (*B*), hippocampus (*D*), superior colliculus (*F*), corpus callosum (*H*), and corticospinal tract (*J*) in the same four groups of mice (mean ± SEM, n = 4–7). The number of perfused (Evans blue$^+$) vessels/mm^2 and total the number of vessels (IB4$^+$)/mm^2 in different brain regions was quantified by an automated counting system. *$P < 0.05$, **$P < 0.01$, ***$P < 0.001$.

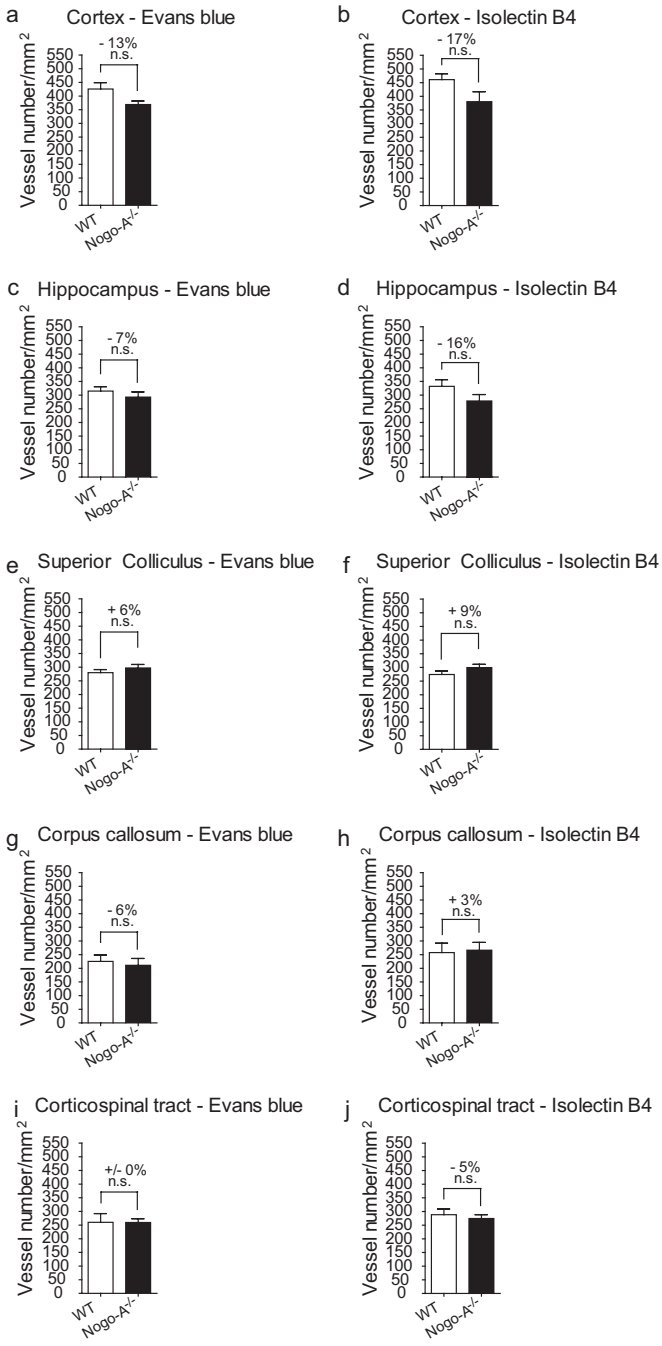

Fig. S4. Nogo-A ablation does not affect the vessel density in the adult brain. Hearts were injected with 2% (wt/vol) Evans blue in 0.9% NaCl (6 μL/g body weight) and were perfused for 5 min before the animals' heads were removed and frozen and 10-μm cryosections were prepared. (*A*, *C*, *E*, *G*, and *I*) Shown are the number of perfused (Evans blue$^+$) vessels per area in adult cortex (*A*), hippocampus (*C*), superior colliculus (*E*), corpus callosum (G), and corticospinal tract (*I*) of WT and Nogo-A$^{-/-}$ mice. Data are shown as mean ± SEM ($n = 4–7$). Nogo-A deletion does not affect the number of blood vessels. (*B*, *D*, *F*, *H*, and *J*) Shown are the number of IB4$^+$ vessel structures in adult cortex (*B*), hippocampus (*D*), superior colliculus (*F*), corpus callosum (*H*), and corticospinal tract (*J*) in WT and Nogo-A$^{-/-}$ mice. Data are shown as mean ± SEM ($n = 4–7$). The number of perfused (Evans blue$^+$) vessels/mm^2 and the total number of vessels/mm^2 (IB4$^+$) in different brain regions were quantified by an automated counting system.

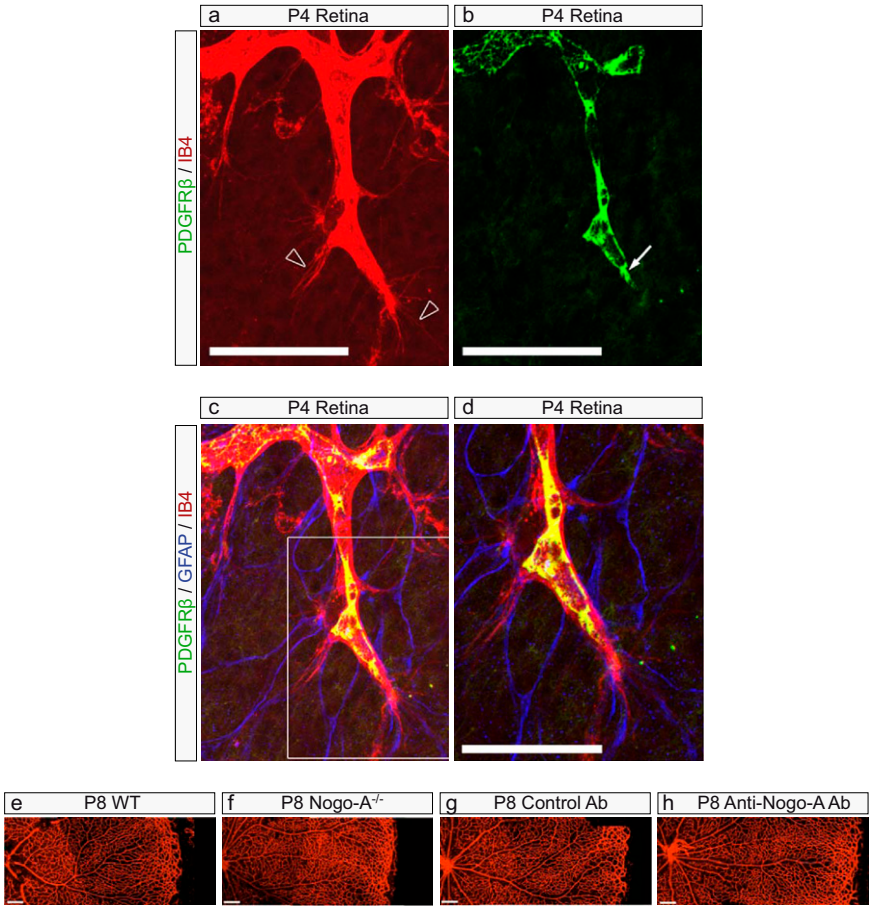

Fig. S5. Detection of pericytes, astrocytes, and endothelial cells in P4 retinas. (*A–D*) Retinal endothelial cells, pericytes, and astrocytes were labeled by immunofluorescence using IB4 (*A*) and antibodies directed against PDGFRβ (*B*) and GFAP (*C*), respectively. The superimposition of the three labelings (*D*) revealed the partial overlap of pericytes and blood vessels at the rear of tip cells, whereas filopodia followed $GFAP^{+}$ extensions. (*E–H*) Superficial retinal vasculature shown by IB4-staining in P8 retinas from WT mice (*E*), Nogo-$A^{-/-}$ mice (*F*), WT mice injected with control antibody (*G*), and WT mice injected with anti–Nogo-A antibody (*H*). No obvious changes in the density of vessel tissue could be observed among the different groups. (Scale bars: 50 μm in *A–C*; 25 μm in *D*; 100 μm in *E–H*.)

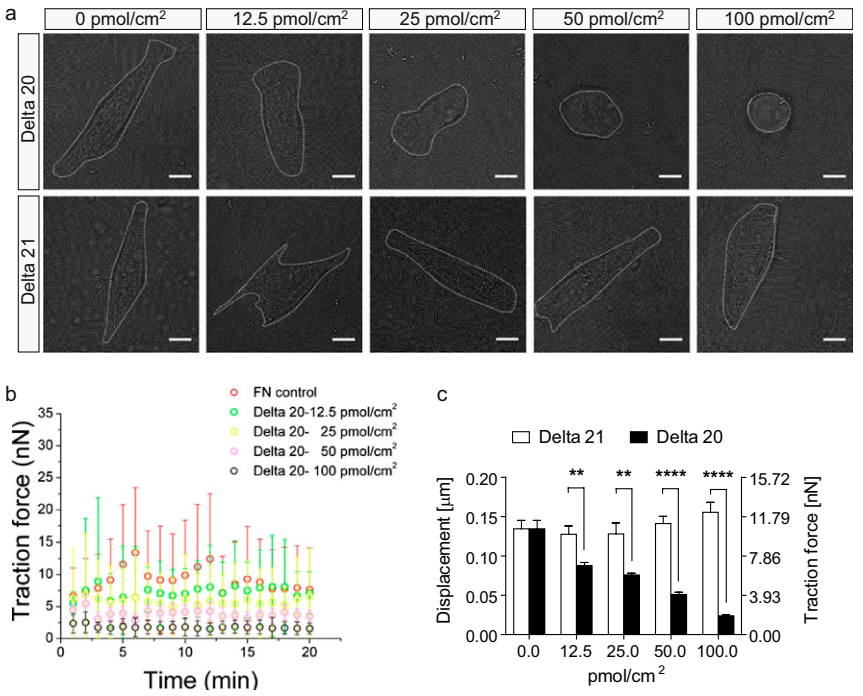

Fig. S6. Nogo-A Delta 20 inhibits MVEC spreading and adhesion on a nanopillar substrate and leads to reduced traction forces between MVECs and nanopillars. (*A*) MVEC spreading was decreased on a substrate consisting of nanopillars coated with increasing concentrations of Nogo-A Delta 20 but not on a substrate of nanopillars coated with Nogo-A Delta 21. White dashed lines outline single MVECs. (Scale bars: 10 μm.) (*B*) Reduced traction forces generated by MVECs on nanopillars coated with Nogo-A Delta 20. For every MVEC at a certain time point, the average of traction forces exerted on the underlying 800–3,200 nanopillars (for Nogo-A Delta 20, depending on the relative concentration) or 3,200 nanopillars (for Nogo-A Delta 21) was calculated. Data shown are mean ± SEM of three MVECs per group ($n = 3$.) (*C*) Displacement and traction force generated by MVECs on nanopillars coated with Nogo-A Delta 20 were dose-dependently decreased compared with MVECs on nanopillars coated with Nogo-A Delta 21. Nanopillars in contact with three individual MVECs were measured for every condition, over a time period of 10 min. Data shown are mean ± SEM of three single MVECs ($n = 3$). $^{**}P < 0.01$, $^{****}P < 0.0001$.

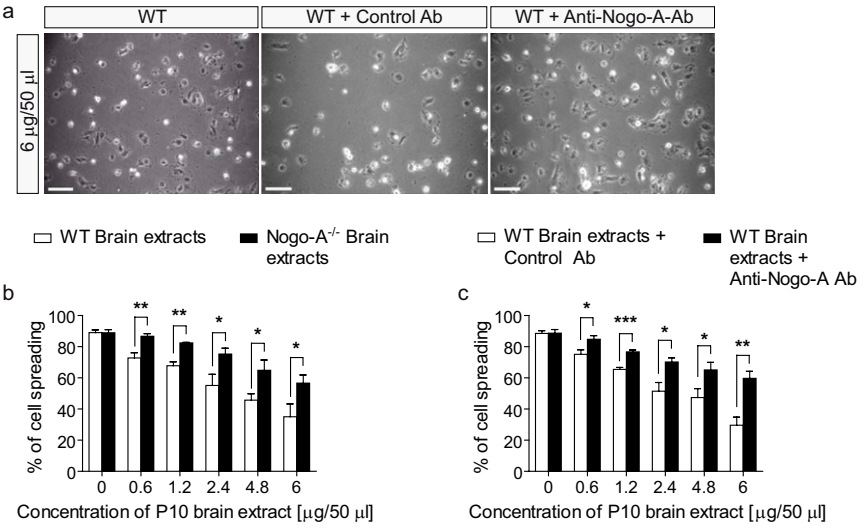

Fig. S7. Nogo-A is a major component of extracts from brain membrane proteins inhibiting MVEC spreading. (*A*) MVEC spreading was decreased on dishes coated with extracts of brain membrane proteins derived from P10 WT animals. Treatment with the neutralizing anti–Nogo-A antibody 11C7 (2, 3) partially reversed the inhibitory effect of the extract. (Scale bars: 100 μm.) (*B* and *C*) MVEC spreading was increased significantly on dishes coated with brain extracts derived from Nogo-A$^{-/-}$ animals (*B*) or on dishes coated with brain extracts from WT animals treated with the neutralizing anti–Nogo-A antibody (*C*) as compared with MVECs on dishes coated with brain extracts from WT animals (*B*) or on dishes coated with brain extracts from WT animals treated with the isotype control antibody (*C*). All data are shown as mean ± SEM of three replica experiments ($n = 3$). $^{*}P < 0.05$, $^{**}P < 0.01$, $^{***}P < 0.001$. (Scale bars: 100 μm.)

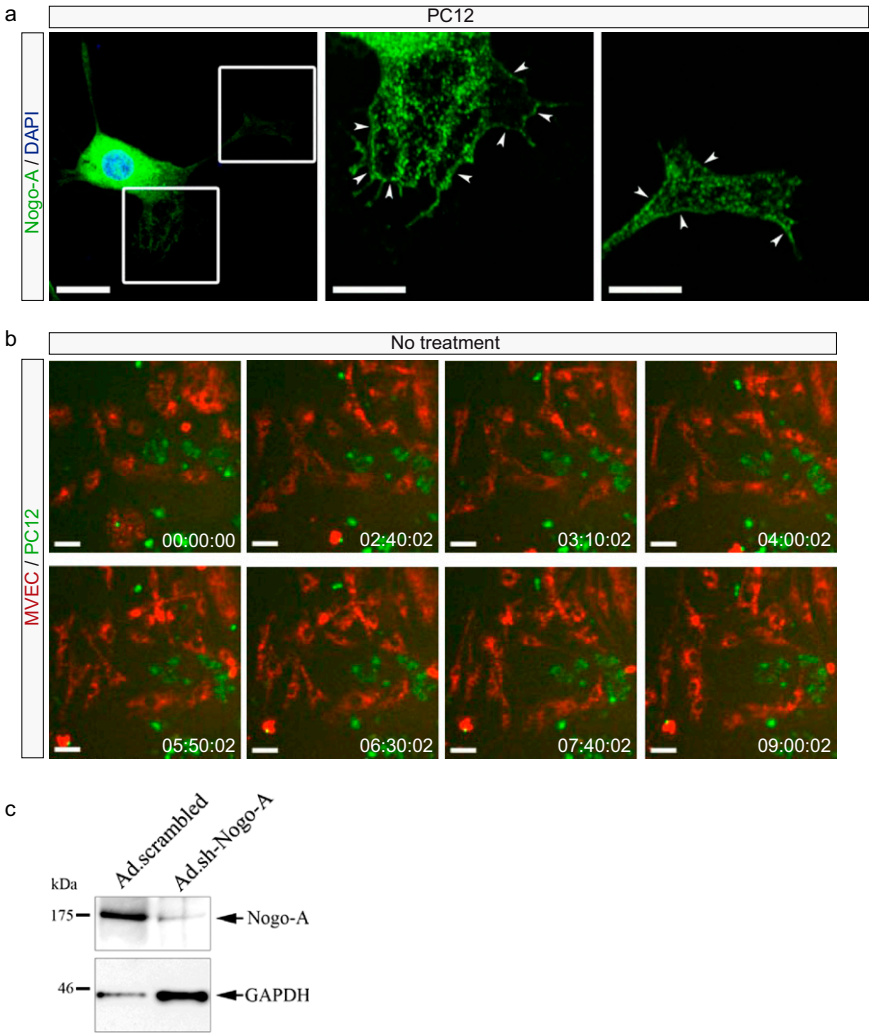

Fig. S8. Nogo-A at the surface of PC12 cells restricts MVEC migration. (*A*) Nogo-A (Laura) is expressed at the membrane of PC12 cells. Boxed areas are enlarged at right. PC12 cells are stained for Nogo-A (Laura) (green) and DAPI (blue). Arrowheads indicate membranous Nogo-A. (*B*) Time course of the formation of a zone of inhibition by PKH26-labeled MVECs (red) around PKH67-labeled PC12 cells (green). Eight frames of Movie S7 are shown. (*C*) Western blot showing Nogo-A (Bianca) (2) down-regulation in PC12 cells infected with Adenovirus small hairpin RNA (Ad.shRNA Nogo-A). No Nogo-A down-regulation was observed in PC12 cells infected with the control virus (Ad.scrambled). (Scale bars: 20 μm in A; 10 μm in the *Insets* in *A*; 50 μm in *B*.)

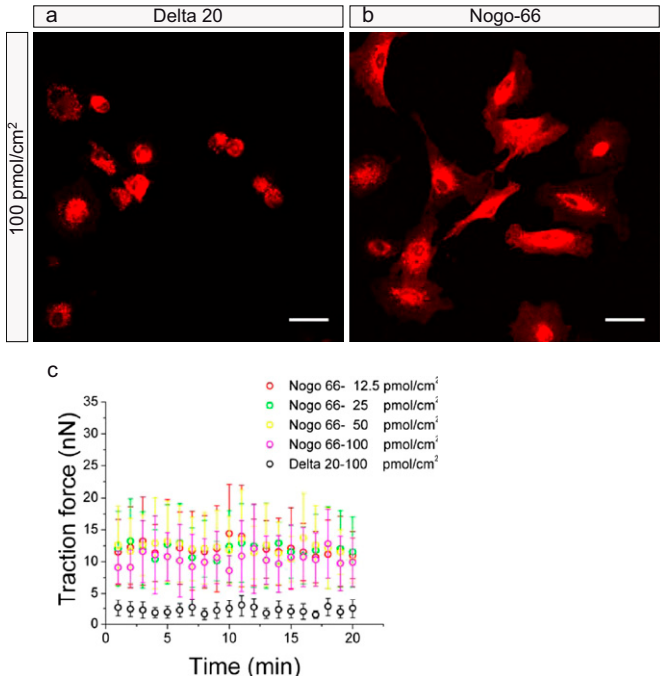

Fig. S9. Nogo-66 does not induce the inhibition of MVEC cell spreading and traction force generation. (*A*) MVEC spreading was decreased on dishes coated with Nogo-A Delta 20 (100 pmol/cm^2). (*B*) MVEC spreading was not inhibited on dishes coated with Nogo-66 (100 pmol/cm^2). (C) Traction forces generated by MVECs on nanopillars coated with Nogo-A 66- were not inhibited, in contrast to MVECs on nanopillars coated with Nogo-A Delta 20. For every MVEC at a certain time point, the average traction force exerted on the underlying ~3,200 nanopillars (for Nogo-66) or ~800 nanopillars (for Nogo-A Delta 20) was calculated. Data shown are mean ± SEM of three MVECs per group (n = 3). (Scale bars: 50 μm.)

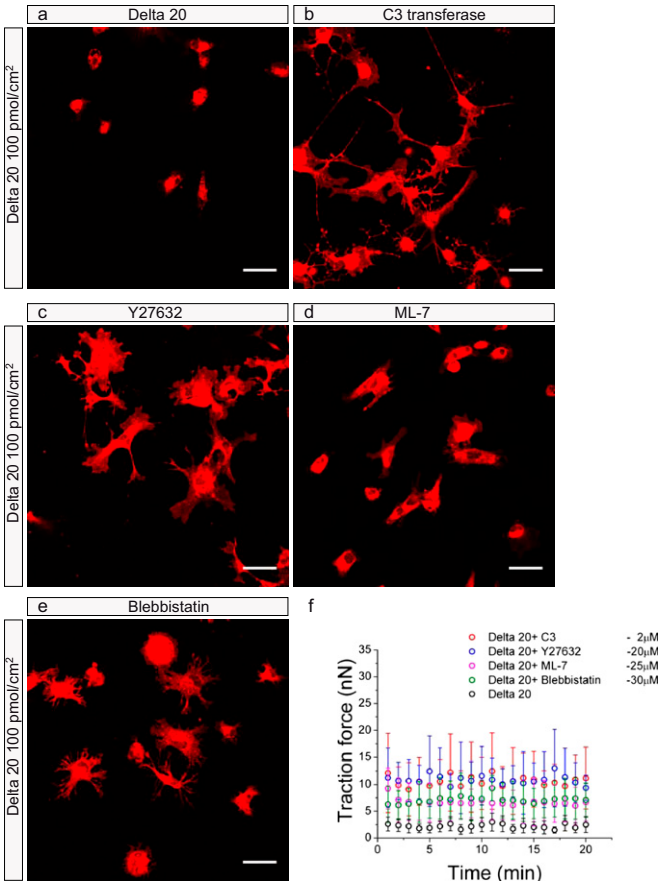

Fig. S10. The Nogo-A Delta 20-induced inhibition of MVEC cell spreading is reversed by inhibitors of Rho, ROCK and Myosin II. (*A*) MVEC spreading was decreased on dishes coated with Nogo-A Delta 20 (100 pmol/cm^2). (*B–E*) Treatment with 2 μM C3 transferase to inhibit Rho (*B*), 20 μM Y27632 to inhibit ROCK (*C*), with 25 μM ML-7 to inhibit MLCK (*D*), and with 30 μM Blebbistatin to inhibit Myosin II ATPase (*E*) prevented the inhibitory effect of Nogo-A Delta 20 on MVEC spreading. (*F*) MVECs treated with the above-mentioned blockers generated increased traction forces on Nogo-A Delta 20–coated nanopillars as compared with untreated MVECs. For every MVEC at a certain time point, the average traction force exerted on the underlying ~800 nanopillars (for Nogo-A Delta 20) or 3,000–5,000 nanopillars (for C3 transferase, Y27632, ML-7, and Blebbistatin) was calculated. Data are shown as the mean ± SEM of three MVECs per group (n = 3.) (Scale bars: 50 μm.)

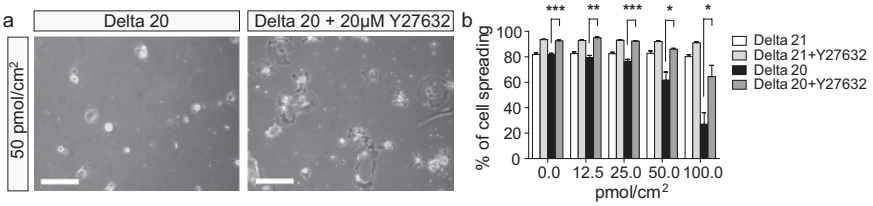

Fig. S11. ROCK inhibition counterbalances the Nogo-A Delta 20-induced inhibition of MVEC cell spreading. (*A*) Treatment with 20 μM of Y27632, the pharmacological inhibitor of ROCK, almost completely prevented the inhibitory effect of Nogo-A on MVEC spreading. (Scale bars: 100 μm.) (*B*) MVEC spreading was increased significantly by Y27632 on a substrate coated with Nogo-A Delta 20. All data are shown as mean ± SEM of three replica experiments (n = 3). *P < 0.05, **P < 0.01, ***P < 0.001.

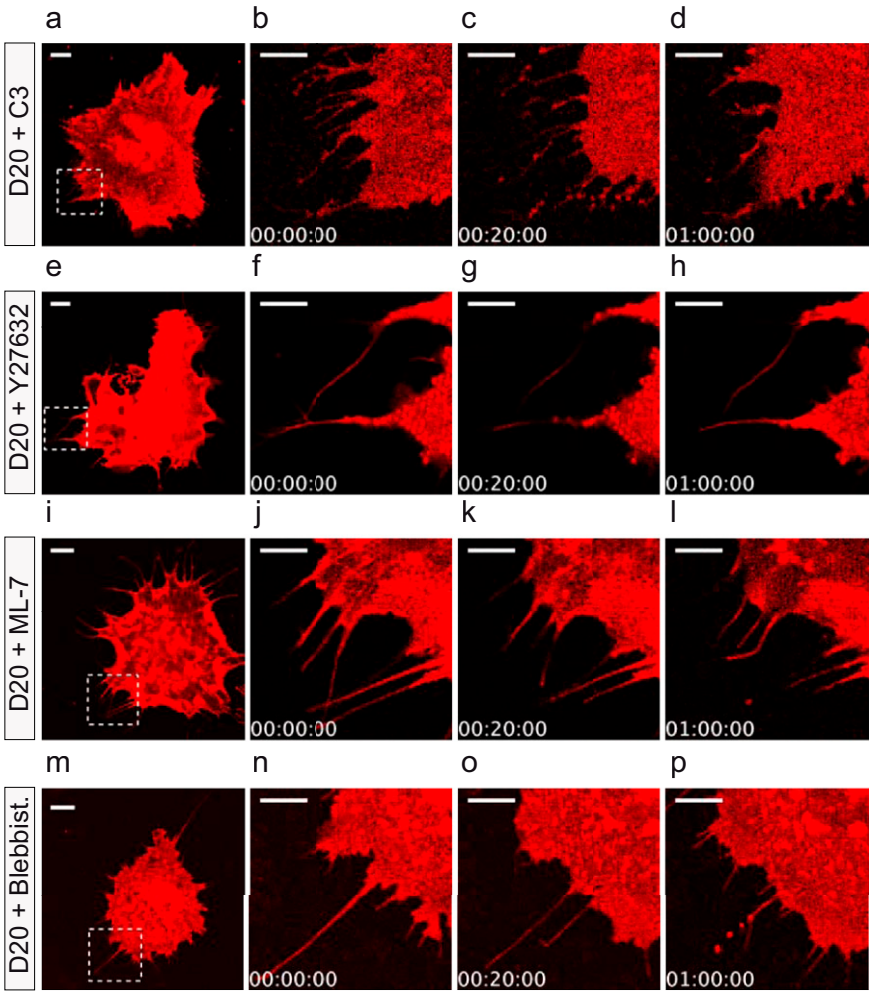

Fig. S12. The Nogo-A Delta 20-induced inhibition of MVEC cell retraction is reversed by inhibitors of Rho, ROCK and Myosin II. Shown are the time courses of DiI-stained P8 MVECs treated with the blockers C3 transferase (2 μM) (*A–D*), Y27632 (20 μM) (*E–H*), ML-7 (25 μM) (*I–L*), and Blebbistatin (30 μM) (*M–P*) and the subsequent addition of 1 μM Nogo-A Delta 20. No retraction of lamellipodia and filopodia could be observed over a 1-h time period. Minor changes in MVEC shape reflecting explorative MVEC behaviors could be seen. Four frames of Movies S15 (*A–D*), S16 (*E–H*), S17 (*I–L*), and S18 (*M–P*) are shown. The boxed areas are enlarged at right. Data are shown as the mean ± SEM of three replica experiments ($n = 3$). (Scale bars: 10 μm in *A*, *E*, I, and *M*; 5 μm in *B–D*, *F–H*, *J–L*, and *N–P*.)

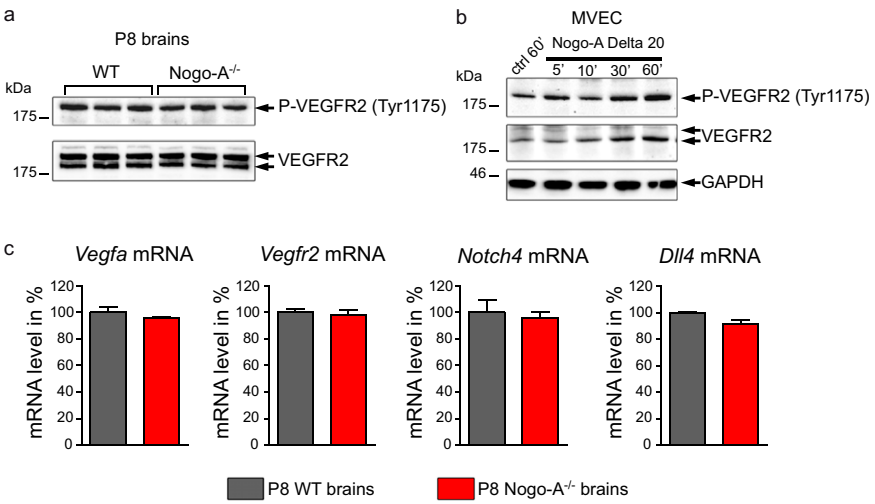

Fig. S13. Nogo-A does not inhibit VEGF signaling in vivo and in vitro. (*A*) The levels of phosphorylated, activated VEGFR2 (P-VEGFR2) and of total VEGFR2 were monitored in P8 Nogo-A$^{-/-}$ mice and P8 WT littermates by Western blotting. No significant change was noticed. Each lane represents 20 μg of whole-brain lysate from individual animals. (*B*) The addition of Nogo-A Delta 20 did not down-regulate VEGFR2 phosphorylation in MVECs. However, a delayed up-regulation of P-VEGFR2 and VEGFR2 levels was detected 30 and 60 min after stimulation, suggesting that VEGFR2 protein synthesis may constitute a late cell response to the stress induced by Nogo-A Delta 20. (*C*) The measurement of *Vegfa*, *Vegfr2*, *Notch4*, and *Dll4* transcripts by quantitative RT-PCR did not show different levels between WT and Nogo-A$^{-/-}$ mouse brains at P8. Three animals were used per condition.

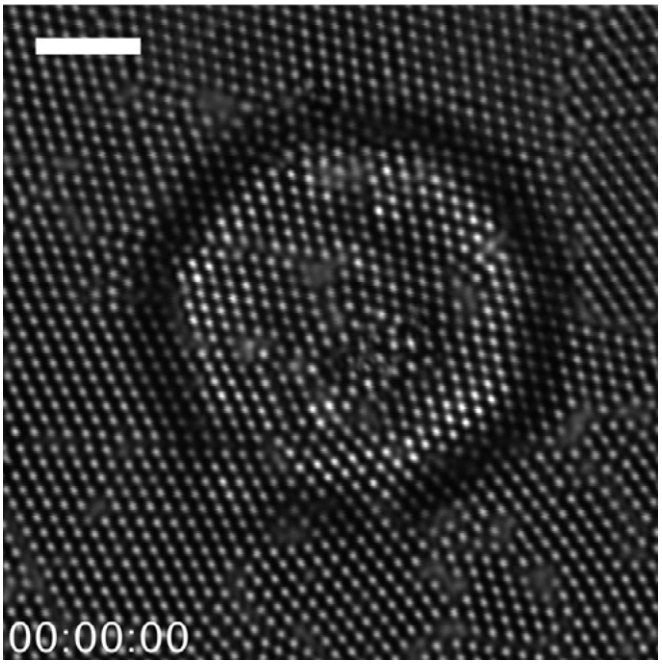

Movie S1. This movie shows a P8 MVEC on a nanopillar substrate coated with Nogo-A Delta 20 (100 pmol/cm^2). Note the inability of the MVEC to spread (i.e., to elaborate lamellipodial and filopodial protrusions) on the inhibitory substrate. The movie represents 29 min (29 frame steps). (Scale bar: 5 μm.)

Movie S1

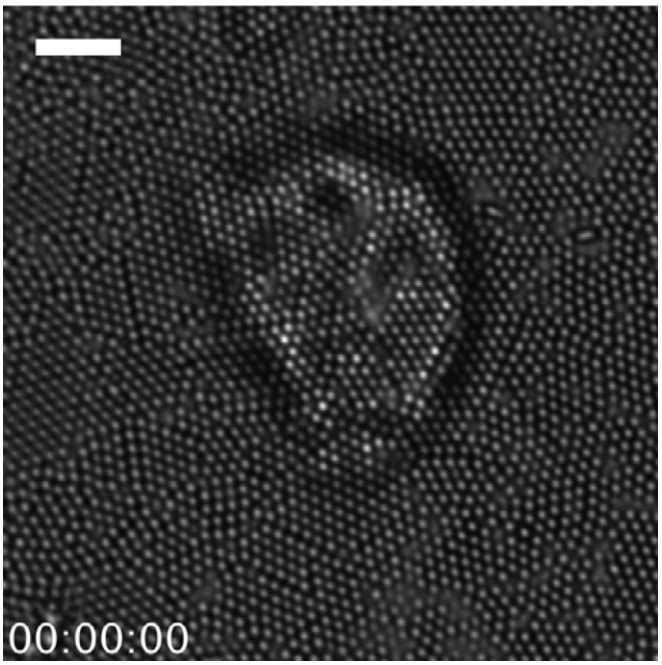

Movie S2. This movie shows a P8 MVEC on a nanopillar substrate coated with Nogo-A Delta 21 (100 pmol/cm^2). Note the MVEC spreading. Elaboration of lamellipodial- and filopodial protrusions can be observed. The movie represents 30 min (30 frame steps). (Scale bar: 5 μm.)

Movie S2

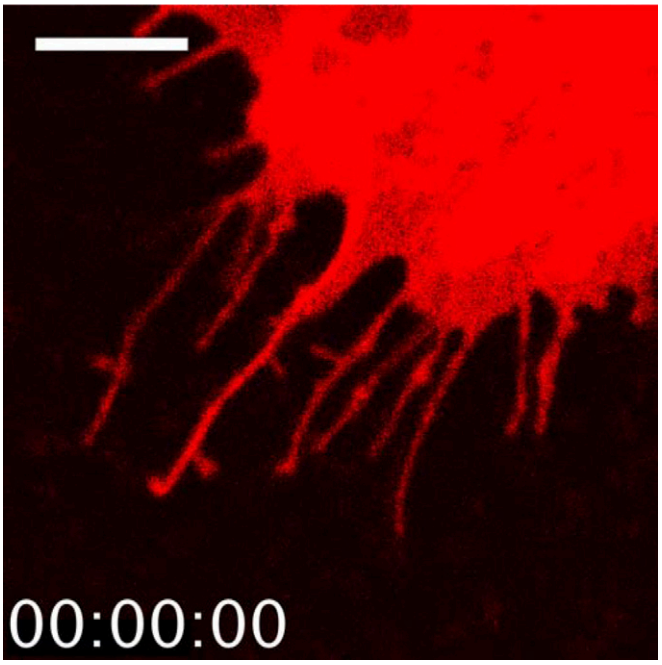

Movie S3. This movie shows a DiI-labeled P8 MVEC on a nanopillar substrate coated with fibronectin (25 μg/mL) after the addition of soluble Nogo-A Delta 20 at a final concentration of 1 μM at time point 0. Note the retraction first of lamellipodia and then of filopodia. The movie represents 90 min (180 frame steps). (Scale bar: 5 μm.)

Movie S3

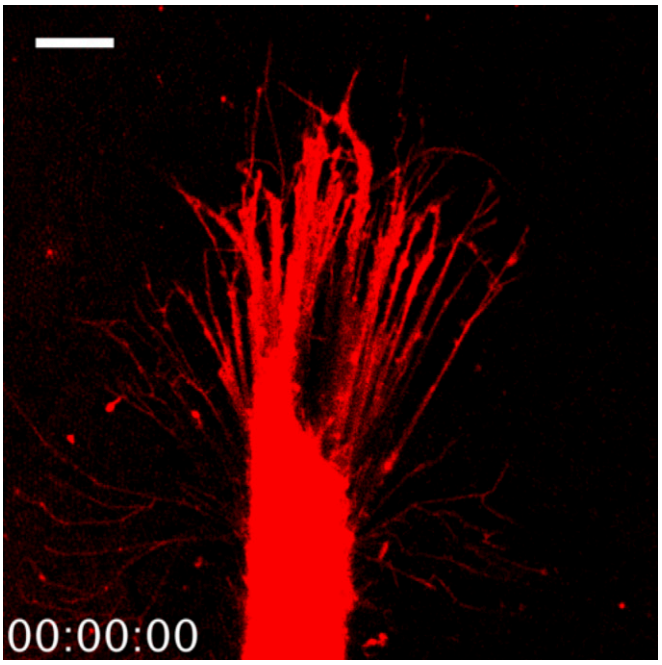

Movie S4. This movie shows a DiI-labeled P8 MVEC on a nanopillar substrate coated with fibronectin (25 μg/mL); soluble Nogo-A Delta 20 at a final concentration of 1 μM was added at time point 0. Note the retraction first of lamellipodia and then of filopodia. The movie represents 106 min (212 frame steps). (Scale bar: 10 μm.)

Movie S4

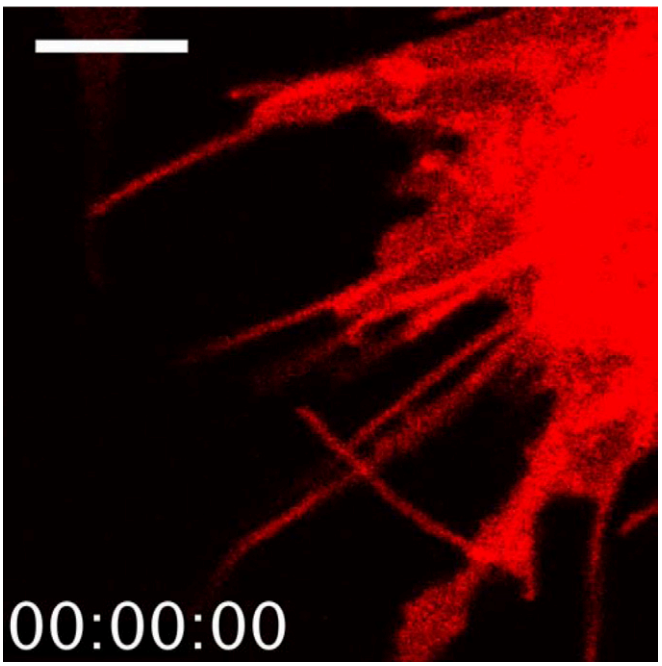

Movie S5. This movie shows a DiI-labeled P8 MVEC on a nanopillar substrate coated with fibronectin (25 μg/mL); soluble Nogo-A Delta 21 at a final concentration of 1 μM was added at time point 0. Note few net displacements of lamellipodia and filopodia. The movie represents 99 min (149 frame steps). (Scale bar: 5 μm.)

Movie S5

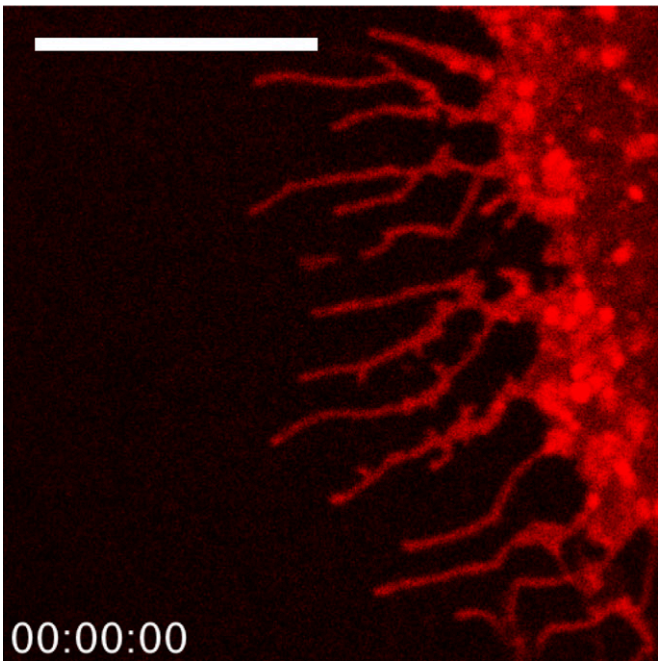

Movie S6. This movie shows a DiI-labeled P8 MVEC on a nanopillar substrate coated with fibronectin (25 μg/mL); soluble Nogo-A Delta 21 at a final concentration of 1 μM was added at time point 0. Note few net displacements of lamellipodia and filopodia. The movie represents 99 min (198 frame steps). (Scale bar: 10 μm.)

Movie S6

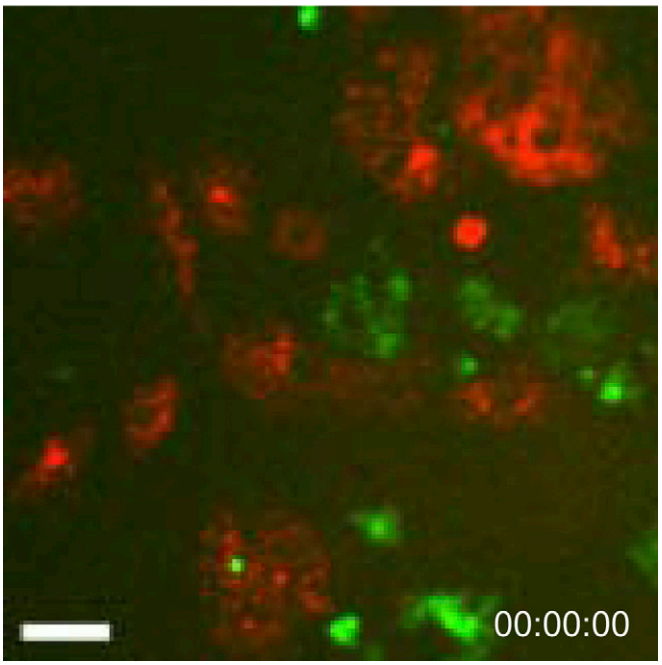

Movie S7. This movie shows the formation of a zone of inhibition of PKH26-labeled P8 MVECs (red) around PKH67-labeled PC12 cells (green) within 9 h after contact of the two cell types. Note the MVEC repulsion after direct contact with PC12 cells. The movie represents 12 h, 30 min, and 2 s (54 frame steps). (Scale bar: 50 μm.)

Movie S7

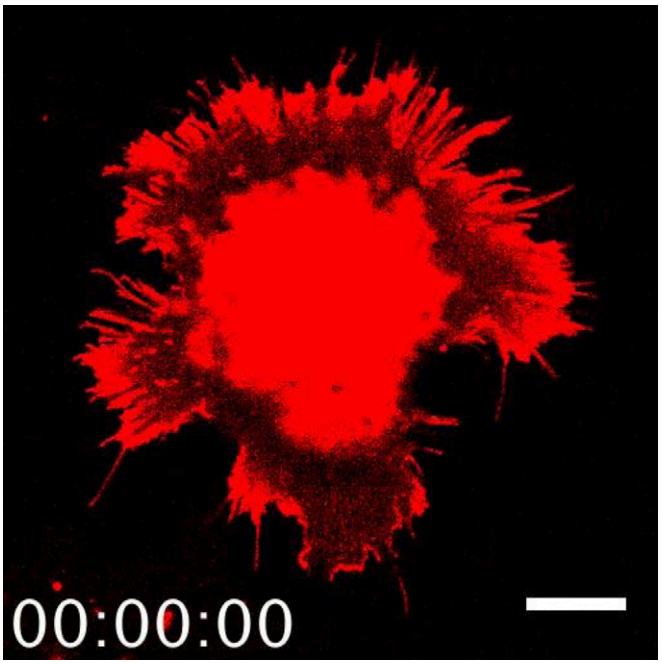

Movie S8. This movie shows a DiI-labeled P8 MVEC on a nanopillar substrate coated with Nogo-66 (100 pmol/cm^2). Note the MVEC spreading. Elaboration of lamellipodial and filopodial protrusions can be observed. The movie represents 24 min (24 frame steps). (Scale bar: 10 μm.)

Movie S8

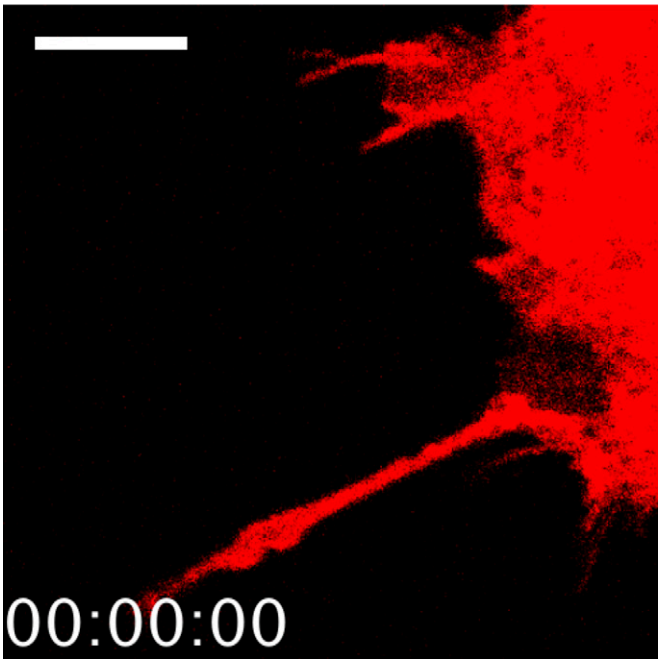

Movie S9. This movie shows a DiI-labeled P8 MVEC on a nanopillar substrate coated with fibronectin (25 μg/mL); soluble Nogo-66 at a final concentration of 1 μM was added at time point 0. Note few net displacements of lamellipodia and filopodia. The movie represents 60 min (30 frame steps). (Scale bar: 5 μm.)

Movie S9

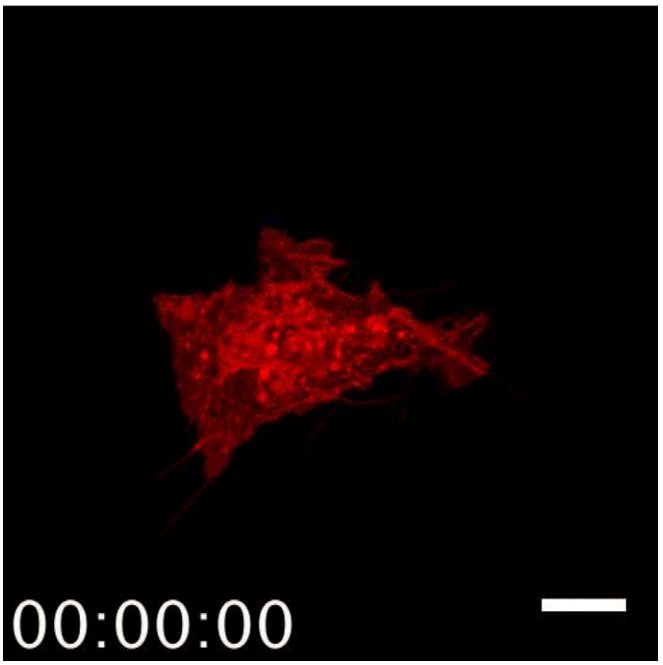

Movie S10. This movie shows a DiI-labeled P8 MVEC on a nanopillar substrate coated with Nogo-A Delta 20 (100 pmol/cm^2). Note the inability of the MVEC to spread (i.e., to elaborate lamellipodial and filopodial protrusions) on the inhibitory substrate. The movie represents 29 min (29 frame steps). (Scale bar: 10 μm.)

Movie S10

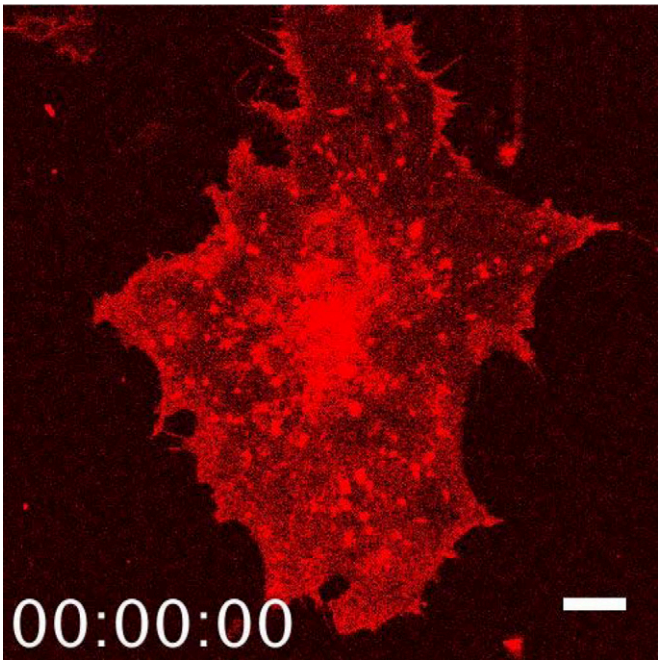

Movie S11. This movie shows a DiI-labeled P8 MVEC on a nanopillar substrate coated with Nogo-A Delta 20 (100 pmol/cm^2). The MVEC was preincubated with C3-transferase (2 μM) for 30 min before culture on the nanopillar substrate. Note few net displacements of lamellipodia and filopodia. The movie represents 24 min (49 frame steps). (Scale bar: 10 μm.)

Movie S11

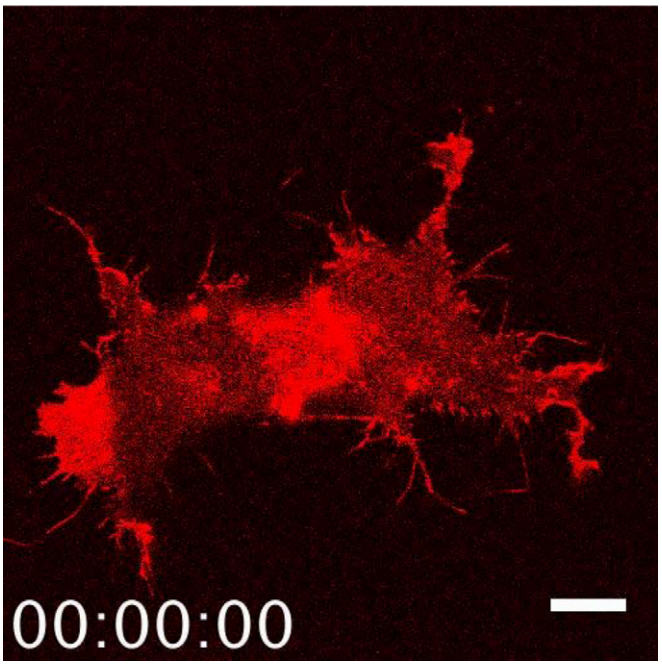

Movie S12. This movie shows a DiI-labeled P8 MVEC on a nanopillar substrate coated with Nogo-A Delta 20 (100 pmol/cm^2). The MVEC was preincubated with Y27632 (20 μM) for 30 min before culture on the nanopillar substrate. Note few net displacements of lamellipodia and filopodia. The movie represents 24 min (49 frame steps). (Scale bar: 10 μm.)

Movie S12

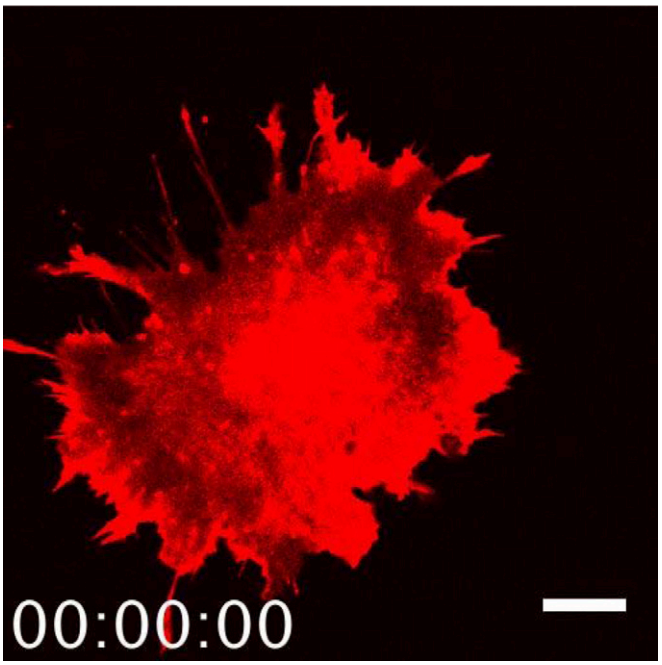

Movie S13. This movie shows a DiI-labeled P8 MVEC on a nanopillar substrate coated with Nogo-A Delta 20 (100 pmol/cm^2). The MVEC was preincubated with ML-7 (25 μM) for 30 min before culture on the nanopillar substrate. Note few net displacements of lamellipodia and filopodia. The movie represents 24 min (49 frame steps). (Scale bar: 10 μm.)

Movie S13

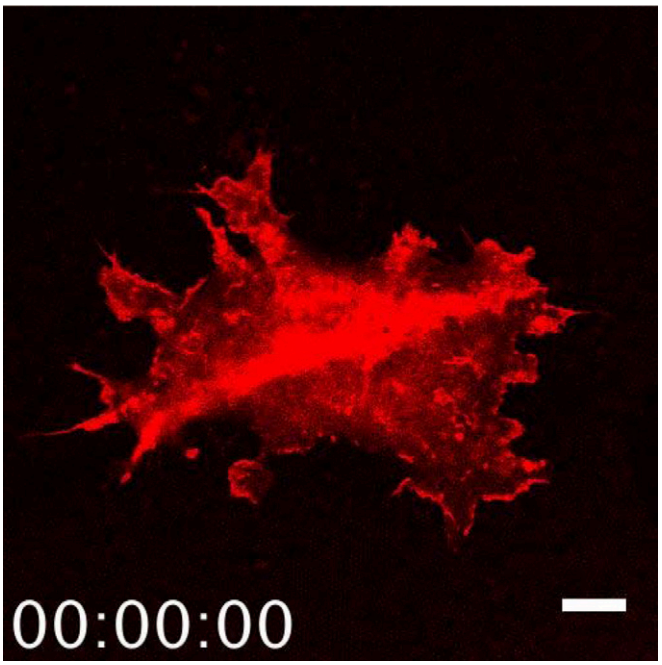

Movie S14. This movie shows a DiI-labeled P8 MVEC on a nanopillar substrate coated with Nogo-A Delta 20 (100 pmol/cm^2). The MVEC was preincubated with Blebbistatin (30 μM) for 30 min before culture on the nanopillar-substrate. Note few net displacements of lamellipodia and filopodia. The movie represents 24 min (49 frame steps). (Scale bar: 10 μm.)

Movie S14

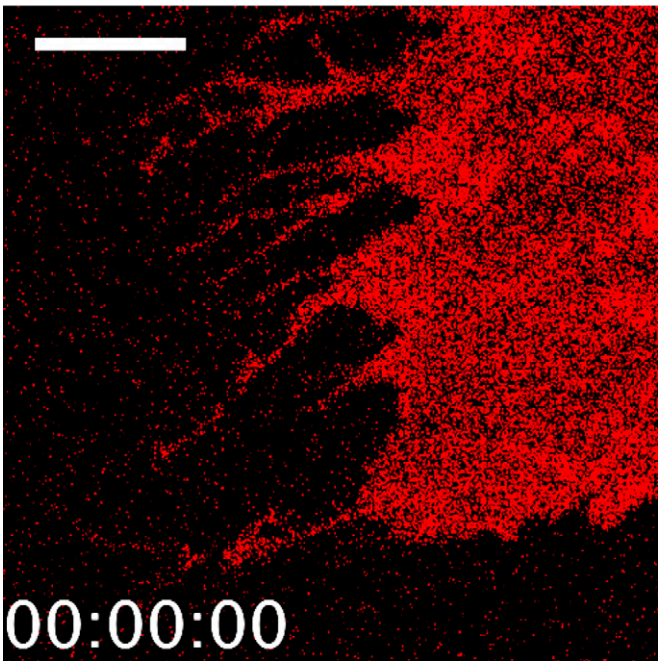

Movie S15. This movie shows a DiI-labeled P8 MVEC on a nanopillar substrate coated with fibronectin-soluble (25 μg/mL); soluble Nogo-A Delta 20 at a final concentration of 1 μM was added at time point 0. The MVEC was cultured for 30 min on the nanopillar substrate and incubated for another 30 min with C3 transferase (2 μM). Thereafter, soluble Nogo-A Delta 20 (1 μM) was added. Note few net displacements of lamellipodia and filopodia. The movie represents 60 min (30 frame steps). (Scale bar: 5 μm.)

Movie S15

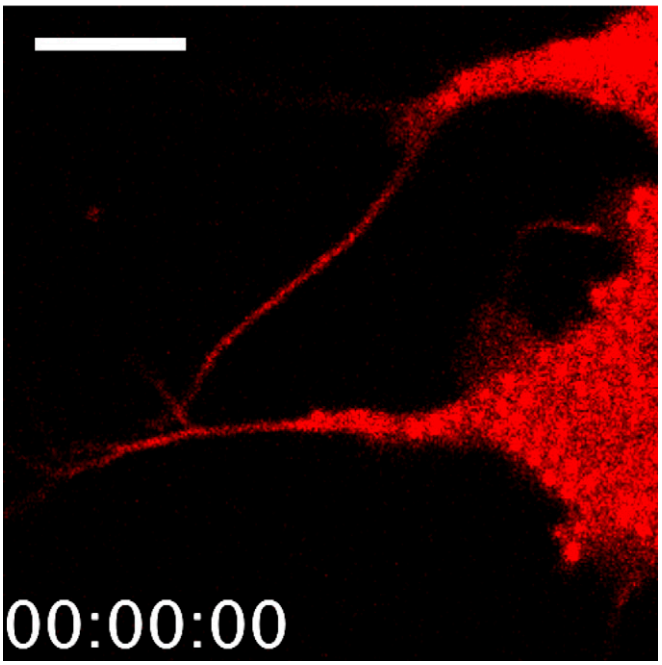

Movie S16. This movie shows a DiI-labeled P8 MVEC on a nanopillar substrate coated with fibronectin (25 μg/mL); soluble Nogo-A Delta 20 at a final concentration of 1 μM was added at time point 0. The MVEC was cultured for 30 min on the nanopillar substrate and incubated for another 30 min with Y27632 (20 μM). Thereafter, soluble Nogo-A Delta 20 (1 μM) was added. Note few net displacements of lamellipodia and filopodia. The movie represents 60 min (30 frame steps). (Scale bar: 5 μm.)

Movie S16

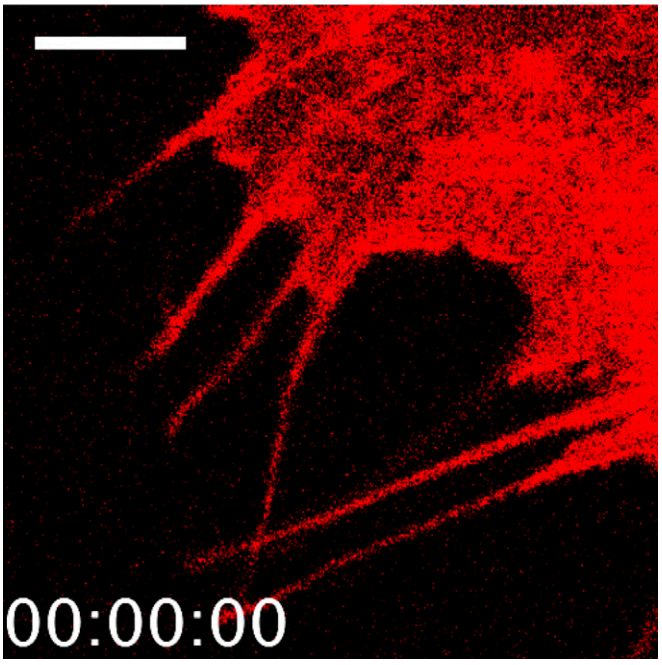

Movie S17. This movie shows a DiI-labeled P8 MVEC on a nanopillar substrate coated with fibronectin (25 μg/mL); soluble Nogo-A Delta 20 at a final concentration of 1 μM was added at time point 0. The MVEC was cultured for 30 min on the nanopillar substrate and incubated for another 30 min with ML-7 (25 μM). Thereafter, soluble Nogo-A Delta 20 (1 μM) was added. Note few net displacements of lamellipodia and filopodia. The movie represents 60 min (30 frame steps). (Scale bar: 5 μm.)

Movie S17

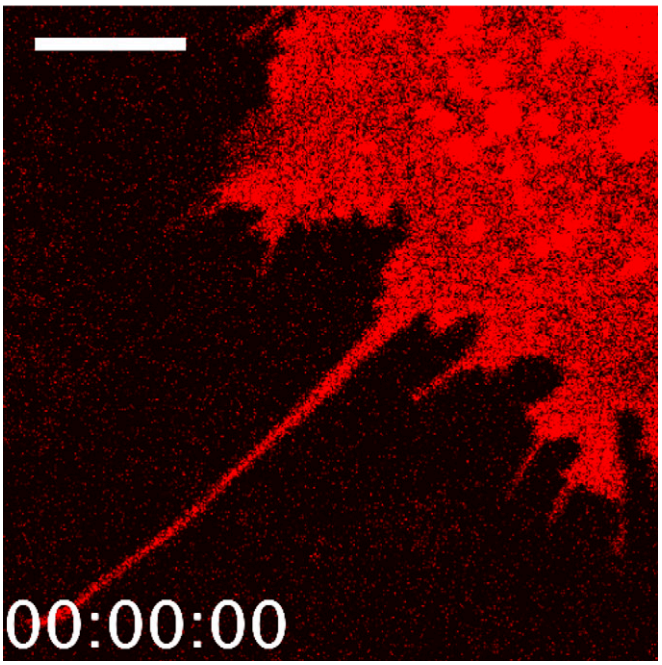

Movie S18. This movie shows a DiI-labeled P8 MVEC on a nanopillar substrate coated with fibronectin (25 μg/mL); soluble Nogo-A Delta 20 at a final concentration of 1 μM was added at time point 0. The MVEC was cultured for 30 min on the nanopillar substrate and incubated for another 30 min with Blebbistatin (30 μM). Thereafter, soluble Nogo-A Delta 20 (1 μM) was added. Note few net displacements of lamellipodia and filopodia. The movie represents 60 min (30 frame steps. (Scale bar: 5 μm.)

Movie S18